ESSSP 2025
地球科學暑期學生
專題研究計畫

Rayleigh Wave Dispersion Analysis Using Broadband Ocean Bottom Seismic Array from the Oldest Pacific Plate

利用寬頻海底地震儀陣列分析太平洋最古老板塊雷利波頻散特性

Hung-Lin Chen[1] and Pei-Ying Patty Lin[2]

陳泓霖[1]　　林佩瑩[2]

[1]chen1061066@gmail.com

國立臺灣師範大學 National Taiwan Normal University
地球科學系 Department of Earth Sciences
行星地震學研究室 Planetary Seismology Laboratory

Introduction & Objectives

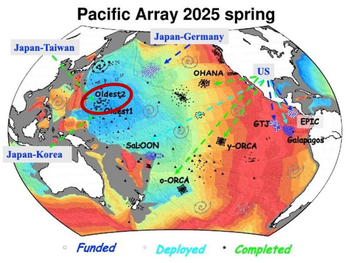

The Pacific Plate, Earth's largest tectonic plate, remains poorly instrumented across its vast oceanic interior. The Pacific Array (Fig. 1) addresses this gap through a multinational deployment of geophysical instruments (Fig. 2) across the entire basin. The Oldest-2 array (Fig. 3) specifically targets ~160 Ma lithosphere east of Guam, providing critical constraints on the long-term evolution of oceanic lithosphere–asthenosphere systems.

Figure 1. Pacific Array seismic network showing the location of the Oldest-2 study area (red circle). Image from https://eri-ndc.eri.u-tokyo.ac.jp/PacificArray/index.html

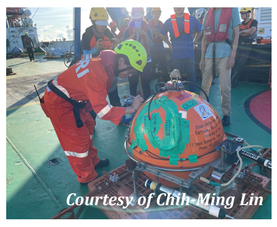

Figure 2. Broadband ocean-bottom seismographs (BBOBSs) deployed in the Oldest-2 array. Two instrument types were used: Taiwan's IES design (left) and Japan's ERI design (right).

Objectives of this study are :

① **Characterize surface wave propagation patterns as a function of period** using seismic array data analysis.

② **Quantify spatial variations in wave velocity** across the study area to identify subsurface heterogeneities.

③ **Determine directional anisotropy** by measuring wave speeds along multiple azimuths and identifying fast propagation directions.

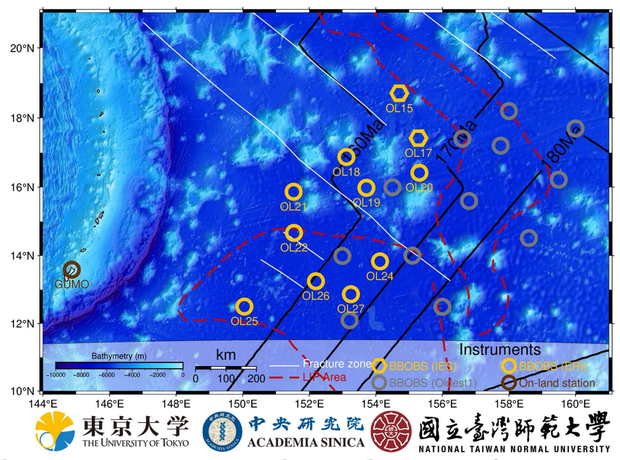

Figure 3. Bathymetric map of the Oldest-2 seismic array in the northwest Pacific Ocean. Seismograph locations: Taiwan IES instruments (hexagons), Japan ERI instruments (circles). Geological features: seafloor age contours (black lines), large igneous provinces (red dashed lines), fracture zones (white lines).

Noise correction for OBS data

(a) Tilt noise

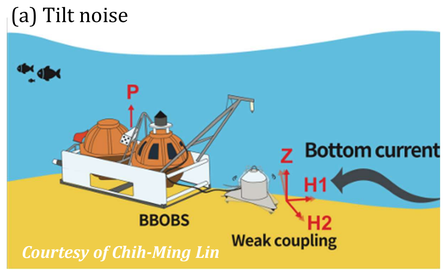

(b) Compliance noise

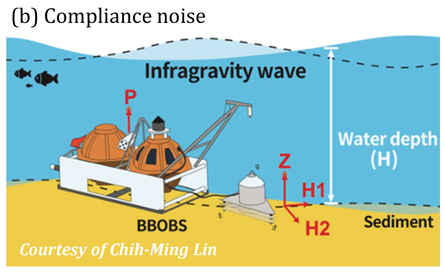

Figure 4. BBOBS noise mechanisms: (a) tilt noise; (b) compliance noise. Tilt noise primarily affects horizontal and vertical components; compliance noise affects pressure and vertical components.

Vertical (Z) components of OBS recordings are affected by two noise mechanisms (Fig. 4): tilt noise resulting from poor instrument-seafloor coupling and ocean currents, and compliance noise generated by long-period infragravity waves that deform the seafloor.

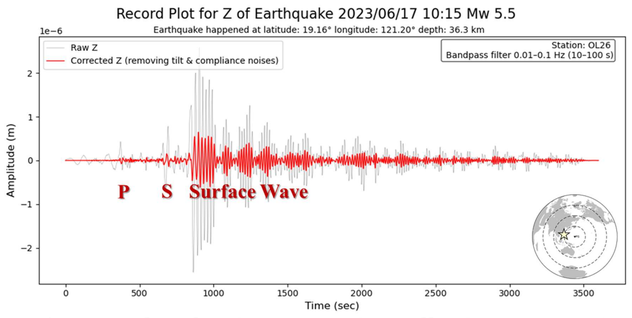

Figure 5. Example of noise correction effectiveness on OBS Z component data. Raw waveform (gray) compared with corrected signal (red) showing improved data quality.

Following noise correction (processed by Isse-san using Kawano et al., 2023 methodology), Z component data quality improves substantially (Fig. 5), enabling accurate Rayleigh wave dispersion analysis.

Measuring the Phase Velocity of Surface Waves

We selected 120 high-quality events (Figure 6) with:

① Time: 2022/09/23 to 2023/10/05

② Magnitude: Mw ≥ 5.5

③ Depth: < 50km

④ Distance: 30° to 120 °

Surface-wave dispersion (Fig. 7) is generally observed as long-period signals arriving earlier than short-period ones. This dispersion shows that wave velocity varies with period. By tracking the same wave peak across multiple stations, the slope of arrival times relative to epicentral distance gives the phase velocity (Fig. 8) for each period.

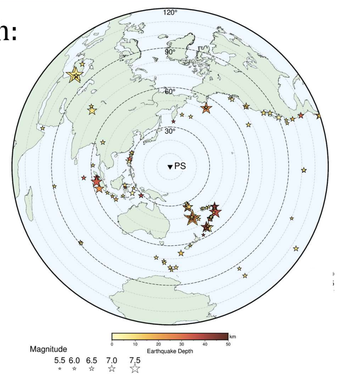

Figure 6. Distribution of teleseismic events used.

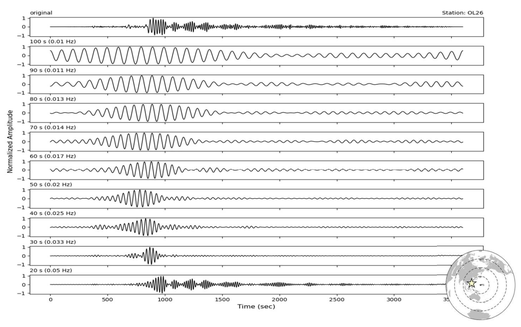

Figure 7. Filtered records showing surface-wave dispersion. Long-period signals (e.g., 80s) arrive earlier, while short-period signals (e.g., 20s) arrive later.

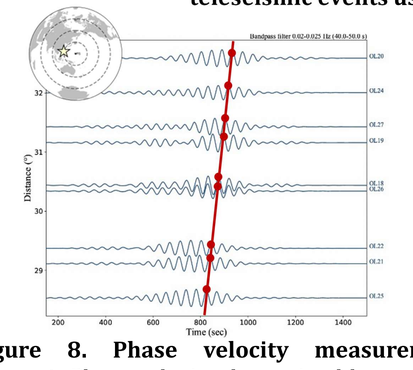

Figure 8. Phase velocity measurement concept. Phase velocity determined by tracking wave peaks across stations. Slope of arrival time versus distance yields phase velocity.

Phase velocities were quantified using cross-correlation analysis (Fig. 9) between station pairs (Jin & Gaherty, 2015). Lag times, combined with epicentral distance differences, provide estimates of phase velocity dispersion (Fig. 10).

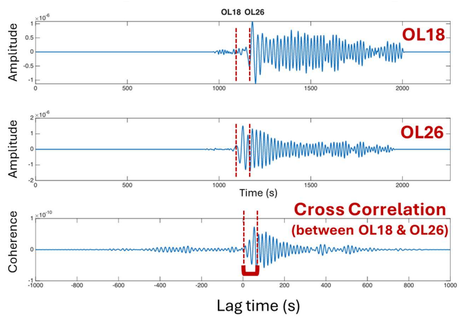

Figure 9. Cross-correlation analysis between two stations. Example showing waveforms recorded at stations OL18 and OL26 and their resulting cross-correlation function.

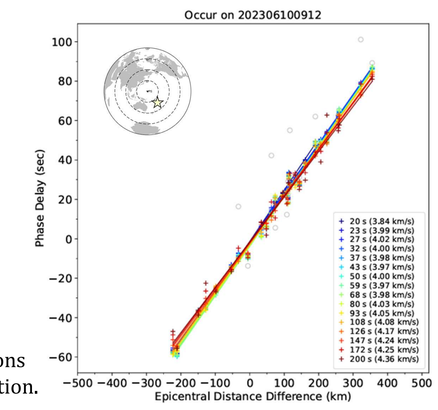

Figure 10. Phase velocity calculation from phase delays. Phase delays at multiple periods versus distance differences for a single event. Slope of each line gives the phase velocity for that period.

Results

Phase velocities and azimuthal anisotropy are simultaneously inverted using least-squares fitting to the functional form: $c(\theta) = c_{iso}[1+A_2\cos(2(\theta-\phi))]$, where is the anisotropy magnitude.

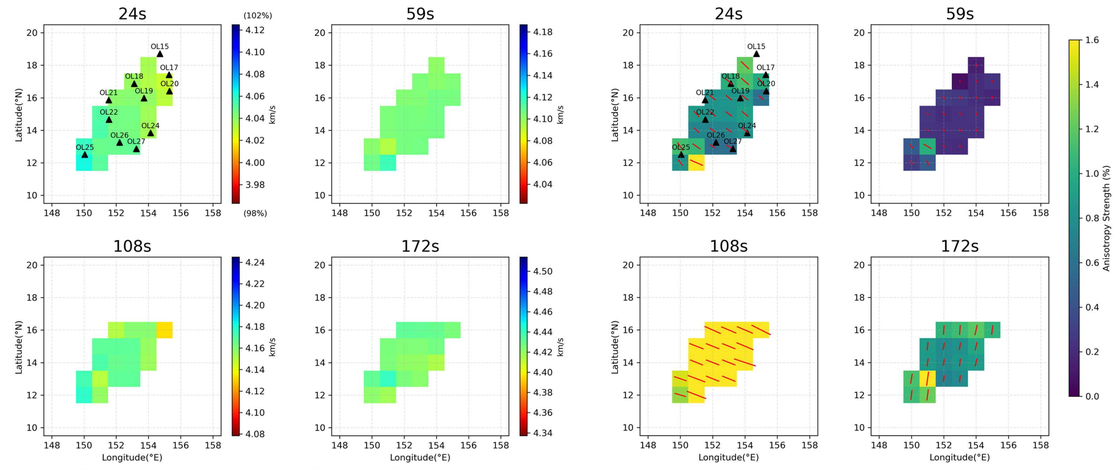

Figure 11. Isotropic phase velocity maps.

Figure 12. Azimuthal anisotropy maps.

Phase velocity tomography yields isotropic maps showing smooth and coherent velocity patterns across the Oldest-2 region (Fig. 11). Subsequent anisotropy analysis (Fig.12) shows that fast directions at short periods (20–60 s) are sub-parallel to the absolute plate motion (APM, 288°), suggesting combined influences from both APM and fossil spreading directions (FSD). At intermediate periods (~108 s), the fast direction aligns with APM and anisotropy strength reaches its maximum. At the longest periods (≥140 s), sampling the deeper asthenosphere, the fast direction rotates to nearly north–south, indicating a distinct deformation regime at depth.

Isotropic phase velocity dispersion curves from raw seismic (LRZ), noise-corrected seismic (LCZ), and pressure (LDH) data show consistent patterns. The dispersion curves demonstrate that Oldest-2 has slower velocities than Oldest-1 (170 Ma) lithosphere (Fig. 13). This confirms that seismic velocities increase with plate age.

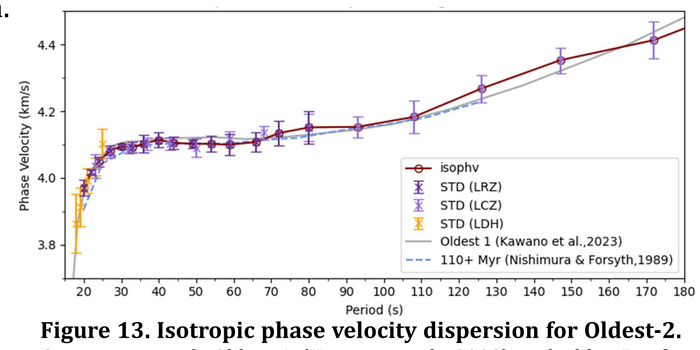

Figure 13. Isotropic phase velocity dispersion for Oldest-2. Comparison with Oldest-1 (Kawano et al., 2023) and older Pacific lithosphere models (Nishimura & Forsyth, 1989).

Key Points & Future Perspectives

- Broadband OBS data from the Oldest-2 array provide new constraints on Rayleigh wave dispersion beneath ~160 Ma Pacific lithosphere.
- Anisotropy analysis shows systematic depth variations: short periods (20-60s) indicate combined plate motion and fossil spreading influences, intermediate periods (~108s) show maximum anisotropy aligned with absolute plate motion, while long periods (≥140s) reveal north-south fast directions and weakening anisotropy at the base of the asthenosphere, demonstrating depth-dependent deformation mechanisms.
- Dispersion analysis confirms that seismic velocities increase with plate age, demonstrating progressive strengthening of Pacific lithosphere.
- Future work will invert dispersion curves for 1-D shear velocity models and expand anisotropy analysis to better constrain fast direction variations and quantify deformation strength with depth.

References & Acknowledgements

Jin, G., & Gaherty, J. B. (2015). Surface wave phase-velocity tomography based on multichannel cross-correlation. Geophysical Journal International, 201(3), 1383-1398. https://doi.org/10.1093/gji/ggv079

Kawano, Y., Isse, T., Takeo, A., Kawakatsu, H., Morishige, M., Shiobara, H., et al. (2023). Seismic structure of the lithosphere-asthenosphere system beneath the oldest seafloor revealed by Rayleigh-wave dispersion analysis. Journal of Geophysical Research: Solid Earth, 128(6). https://doi.org/10.1029/2023jb026529

Nishimura, C. E., & Forsyth, D. W. (1989). The anisotropic structure of the upper mantle in the Pacific. Geophysical Journal International, 96(2), 203–229. https://doi.org/10.1111/j.1365-246X.1989.tb04446.x

NSTC 國科會 · IES 地球科學研究所 · TORI 台灣海洋科技研究中心 · 勵進 · IRIS · MATLAB · python · PyGMT · ObsPy A Python Framework for Seismology